

The Bipolar Resistive Switching in BiFeO₃ Films

Qingyu Xu · Xueyong Yuan · Mingxiang Xu

Received: 5 October 2011 / Accepted: 29 November 2011 / Published online: 21 December 2011
© Springer Science+Business Media, LLC 2011

Abstract Pure-phase polycrystalline BiFeO₃ films have been successfully prepared by pulsed-laser deposition on surface oxidized Si substrates using LaNiO₃ buffer layer with substrate temperature (T_s) ranging from 550 °C to 800 °C and a laser frequency of 5 Hz and 10 Hz. Bipolar resistive switching has been observed in all the films using LaNiO₃ as bottom electrodes and silver glue dots as top electrodes, the resistivity switches from a high-resistance state (HRS) to a low-resistance state (LRS) with positive voltage applied on the top Ag electrodes, and from LRS to HRS with positive voltage applied on the bottom LaNiO₃ electrodes. The mechanism of the resistive switching has been confirmed to be due to the voltage polarity dependent formation/rupture of the conducting filaments formed by the O vacancies. The highest resistive ratio of HRS to LRS, of more than 2 orders of magnitude, has been achieved in the highest resistive BiFeO₃ film prepared at T_s of 650 °C and laser frequency of 10 Hz.

Keywords Multiferroic · Resistive switching · Defects

1 Introductions

Chua noted the missing element in 1971, called memristor, with memristance M having a functional relation between charge and flux, $d\varphi = Mdq$, which has been discovered in Pt/TiO₂/Pt sandwich device later in 2008 [1]. As stated in

the review of Chua, all 2-terminal non-volatile memory devices based on resistive switching (RS) are memristors, regardless of the device material and physical operating mechanism [2]. Based on the dependence of the operating voltage polarity, the RS can be classified as bipolar RS (BRS) and unipolar RS (URS) [3]. Both BRS and URS have been observed in various materials, especially oxides, including binary oxides, such as ZnO [4], SnO₂ [5], Co₃O₄ [6], NiO [7], and perovskites such as SrTiO₃ [8], Pr_{0.7}Ca_{0.3}MnO₃ [9], etc.

BiFeO₃ is the most widely studied multiferroic materials due to its above room temperature antiferromagnetic Neel temperature ($T_N \sim 643$ K) and ferroelectric Curie temperature ($T_C \sim 1103$ K) [10]. Large spontaneous polarization of over 60 $\mu\text{C}/\text{cm}^2$ has been observed in high-quality epitaxial BiFeO₃ films [10], single crystals [11], and even polycrystalline films [12]. The large leakage current is always the main obstacle to observe the well shaped ferroelectric hysteresis loop with large spontaneous polarization [13]. However, as indicated by Yin, the leakage current on the other hand can be used to some extent in some applications, such as non-volatile resistive random access memory [14]. BRS and URS have been both observed in BiFeO₃ films [14–18], however, the mechanism is still under debate. Yin attributed the BRS to the redistribution of the O vacancies in grain boundaries [14]. Li attributed the BRS to the formation/rupture of the nanoscale metal filaments due to the diffusion of the top electrodes under the bias voltage [15]. Shuai observed the BRS in Au/BiFeO₃/Pt structure, which originated from the electric field-induced carrier trapping and detrapping which changes the depletion layer thickness at the Au/BiFeO₃ interface [16]. Chen reported the BRS in BiFeO₃ film and attributed to the modification of the Schottky barrier height at Pt/BiFeO₃ interface due to the movement of O vacancies under electric fields [17]. Chen ob-

Q. Xu (✉) · X. Yuan · M. Xu
Department of Physics, Southeast University, Nanjing 211189,
China
e-mail: xqingyu@seu.edu.cn

served URS in BiFeO₃ film, and the conducting filaments were formed by the O vacancies [18]. The resistive switching is not only depend on the material itself, but also the interface between the electrode and the material, e.g. for Mn-doped ZnO film, URS has been observed with Pt as top electrode while BRS with Si as top electrode [19]. In this paper, we report the BRS in BiFeO₃ films with LaNiO₃ as buffer layer and bottom electrode, and silver glue dots as top electrode. The resistive switching has been demonstrated to be due to the voltage polarity dependent formation/rupture of the conducting filaments formed by the O vacancies.

2 Experimental Details

BiFeO₃ films have been deposited on surface oxidized Si substrates at different substrate temperatures T_s (550 °C, 600 °C, 650 °C, 700 °C, 750 °C and 800 °C) by pulsed-laser deposition (PLD) using a KrF excimer laser with frequency of 5 Hz and 10 Hz from an analytically pure Bi_{1.04}FeO₃ target. Before the deposition of BiFeO₃ film, LaNiO₃ buffer layer was first deposited at T_s of 850 °C in an O₂ ambient with pressure of 40 Pa. The O₂ pressure during the deposition of BiFeO₃ films was kept to be 2 Pa. Then the O₂ pressure was increased to 1×10^5 Pa. The T_s decreased to 550 °C and the samples were annealed for 30 min. The film thickness was controlled by the number of laser pulses (1000 in this paper) with pulse energy of 250 mJ. The thickness of LaNiO₃ and BiFeO₃ layers was estimated by the transmission electron microscopy (TEM) to be about 30 nm and 70 nm, respectively. The structure of the film was studied by X-ray diffraction (XRD, Rigaku SmartLab(3)). The current–voltage (I – V) measurements were carried out using a Keithley 2400 SourceMeter and 2182A Nanovoltmeter at room temperature. Silver glue dots with a diameter of ca. 1 mm were used as top electrodes. During the voltage sweep mode, the bias was defined as positive when the current flowed from the top Ag electrode through the film to the bottom LaNiO₃ electrode.

3 Results and Discussion

Pure-phase BiFeO₃ is difficult to obtain due to the narrow synthesis area in the phase diagram [20]. To obtain pure-phase BiFeO₃ films, appropriate substrate or buffer layer should be selected. If we deposited BiFeO₃ films on surface oxidized Si substrates directly, the films exhibited nearly amorphous structure at low T_s and high concentration of impurity phases at high T_s . LaNiO₃ has been used successfully as buffer layer for the preparation of BiFeO₃ film [17, 21]. With LaNiO₃ as buffer layer, there is a wide T_s window for the preparation of pure-phase BiFeO₃ films. As can be seen

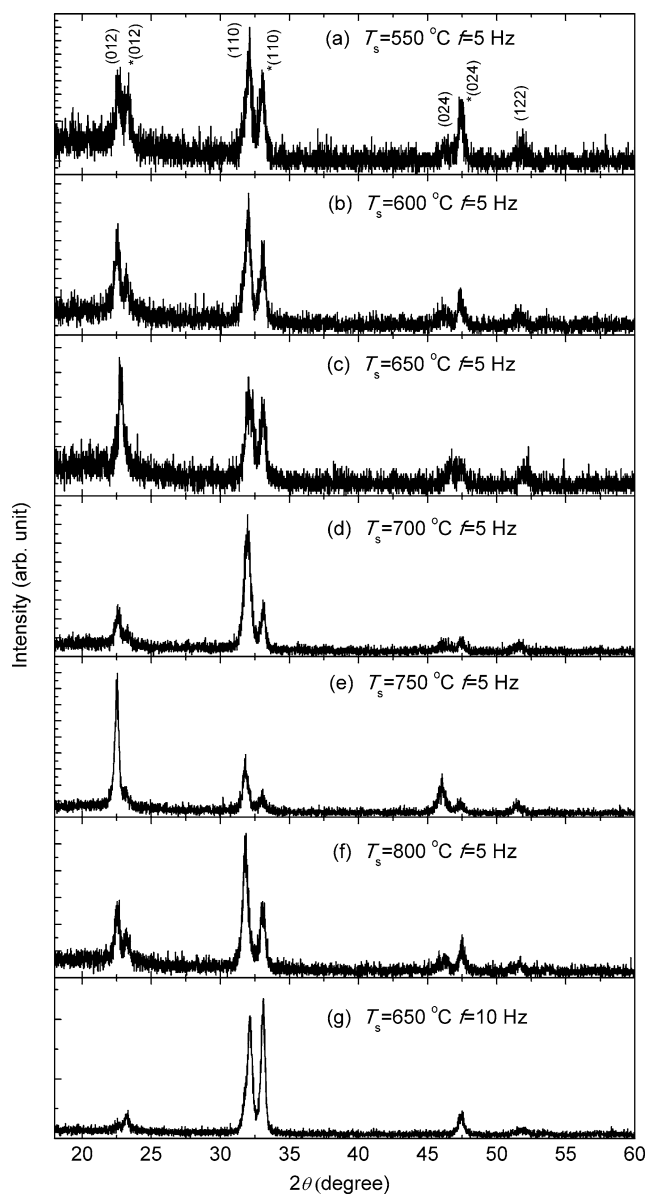


Fig. 1 XRD patterns of the BiFeO₃ films prepared under different conditions. The star “*” indicates the diffraction peaks from LaNiO₃ buffer layer

in Fig. 1, all the BiFeO₃ films prepared at T_s from 550 °C to 800 °C exhibit pure R3c structure without any impurity phase. The crystal orientation of the BiFeO₃ film varied with different T_s . The BiFeO₃ film exhibited preferred (012) orientation at T_s of 650 °C and 750 °C. The crystal orientation was also influenced by the laser frequency. As can be seen, the relative intensity of (012) peak was strongly suppressed at T_s of 650 °C with laser frequency changed from 5 Hz to 10 Hz.

The substrate temperature has a strong influence on the leakage current of the BiFeO₃ films. Figure 2 shows the I – V curves with positive bias before the measurements of the resistive switching. As can be seen, the leakage current

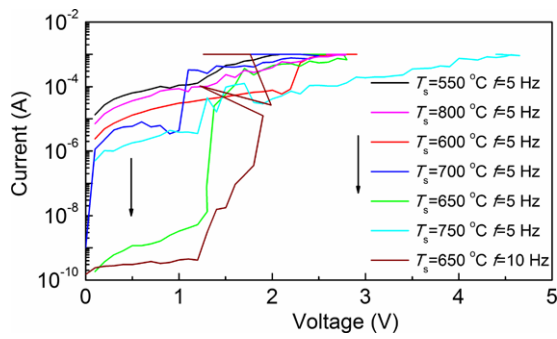


Fig. 2 The forming I – V curves for BiFeO₃ films prepared under different conditions

was strongly suppressed at T_s of 650 °C, while the BiFeO₃ films prepared at higher T_s or lower T_s are all leakage. Recently, Shuai has reported that with higher laser frequency, the leakage current of BiFeO₃ film can be efficiently suppressed and well shaped ferroelectric hysteresis loop with large spontaneous polarization can be achieved [12]. This has been confirmed by our experiment. As can be seen in Fig. 2, the leakage current of BiFeO₃ film prepared at T_s of 650 °C with laser frequency of 10 Hz was further suppressed compared with the BiFeO₃ film prepared at T_s of 650 °C with laser frequency of 5 Hz.

After an initial forming process, stable BRS can be observed in all the films. This is in contrast to the previous reports that the BRS can only be observed in the BiFeO₃ films annealed at temperature higher than 650 °C [14], which might be due to the better crystal quality of the BiFeO₃ films prepared by PLD at low T_s with LaNiO₃ as buffer layer than by chemical solution deposition. As can be seen in Fig. 3, with positive bias applied, the resistance of all the BiFeO₃ films switched from the HRS to the LRS, and switched from the LRS to the HRS with negative bias applied. In contrast to the continuous variation of the current in dependence on the applied bias due to the interface effect such as modification of the depletion width [16], a sudden increase of current in positive bias and decrease of current in the negative bias can be observed, indicating the formation of the conducting filaments. Multiple steps can be observed with sudden increase of current in positive bias and sudden decrease of current in negative bias, indicating the formation of multiple filaments [22, 23].

To confirm the BRS behavior, we also applied the bias in the same direction as the voltage applied to switch the resistance from HRS to LRS. As can be seen in Fig. 4(a), the current continued to increase and no switching from LRS to HRS was observed with bias applied up to 10 V. After that, a hard break happened and no BRS can be observed. Thus the switching from HRS to LRS and from LRS to HRS depends on the polarity of the applied bias.

To further understand the conducting mechanism, the I – V curves have been fitted by several models, including the

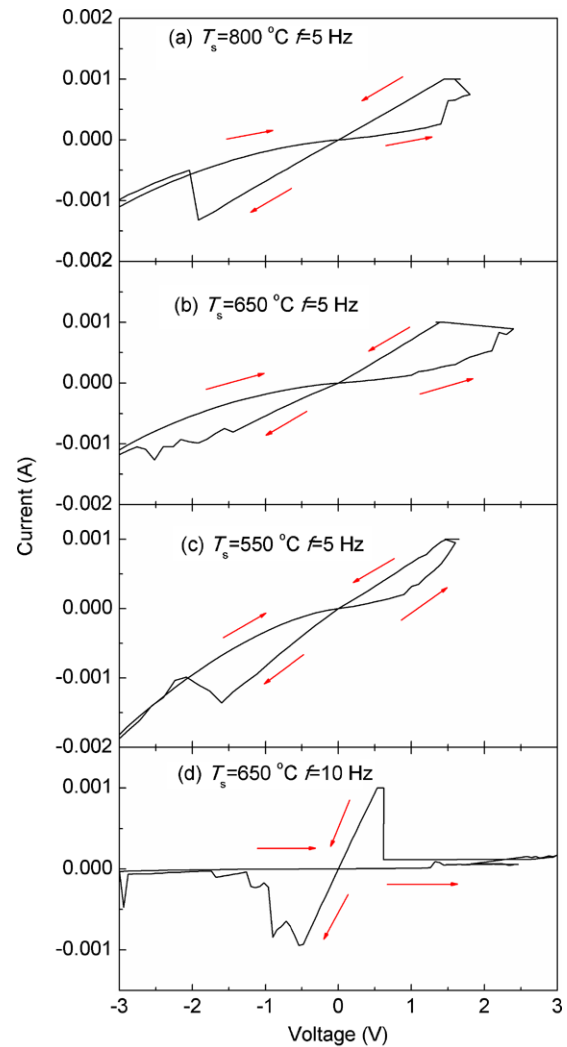


Fig. 3 Typical BRS characteristics of BiFeO₃ films prepared under different conditions. The arrows indicate the voltage applied sequence

Ohmic law ($I \propto V$), space charge limited current (SCLC) ($I \propto V^2$), Schottky emission ($\ln(I) \propto \text{Sqrt}(V)$), Poole–Frenkel (PF) emission ($\ln(I/V) \propto \text{Sqrt}(V)$), and Fowler–Nordheim tunneling ($\ln(I/V^2) \propto 1/V$) [24]. Double logarithmic plots of the I – V curves in both LRS and HRS states are presented in Fig. 5. An I – V characteristic in LRS displays the Ohmic behavior with approximate slope of 1. The conduction mechanism of the HRS at the low voltage is also close to 1, following Ohm’s law. And a quadratic dependence of the current on voltage displays at higher voltage in HRS with slope close to 2. This conduction behavior in HRS is well consistent with the trap-controlled space charge limited conduction (SCLC) mechanism [17, 24]. The slight deviation of the slope from 2 at higher voltage in HRS might be due to the deep-level traps [25]. We also fitted the I – V curves by other mechanisms, but the fitting results were not good (not shown here). Thus, the resistive switching can be

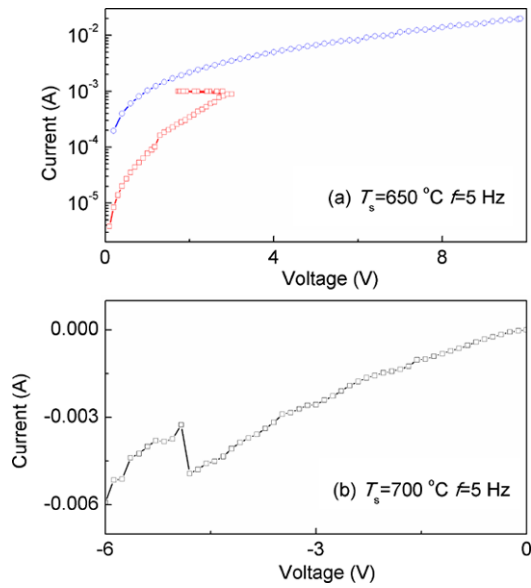
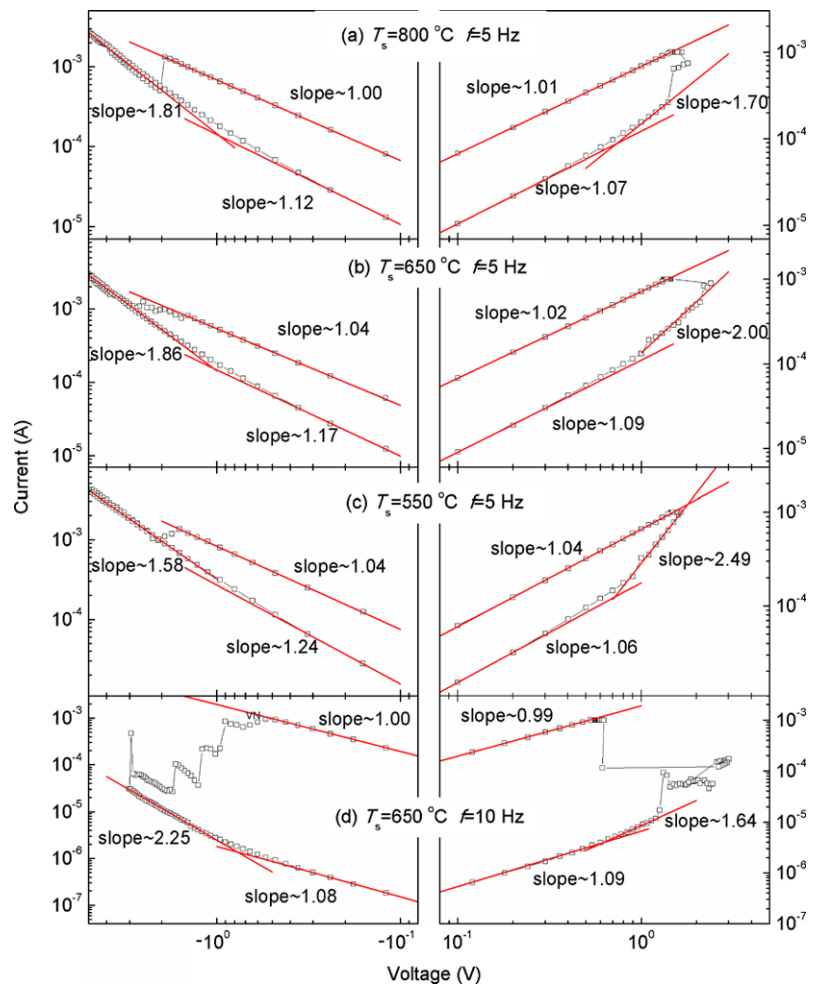


Fig. 4 (a) The set and reset I - V curves with positive applied bias, (b) the forming I - V curve with negative applied bias

explained by the formation/rupture of the conducting filaments [26].

The conducting filaments might be formed by the migration of the O vacancies [14], or the metal atoms from the top electrodes [15]. Ag^+ might migrate from Ag electrode to the counter electrode and reduce there, the successive precipitations of Ag metal atoms will form the conducting filaments [26]. As can be seen in Fig. 4(b), the forming process with negative bias switched from the LRS to HRS. As in the initial state, there should be no Ag atom in the film, thus the conducting filaments formed by Ag atoms can be excluded. At low T_s , the film has smaller grains with high concentration of the grain boundaries. The distribution and redistribution of O vacancies in grain boundaries are responsible for the formation/rupture of the conducting filaments [14]. At high T_s , larger grains with less grain boundaries and better crystal quality can be achieved. However, the Bi concentration in the deposited BiFeO_3 films prepared by PLD decreased with increasing T_s due to the evaporation of Bi during deposition [27]. At T_s above 700°C , the Bi concentration is below the stoichiometric composition [27]. For the charge balance, O vacancies will form. The physical mechanism of the BRS is still under investigation. Generally the

Fig. 5 The log-log plot of I - V curves for BiFeO_3 films prepared under different conditions



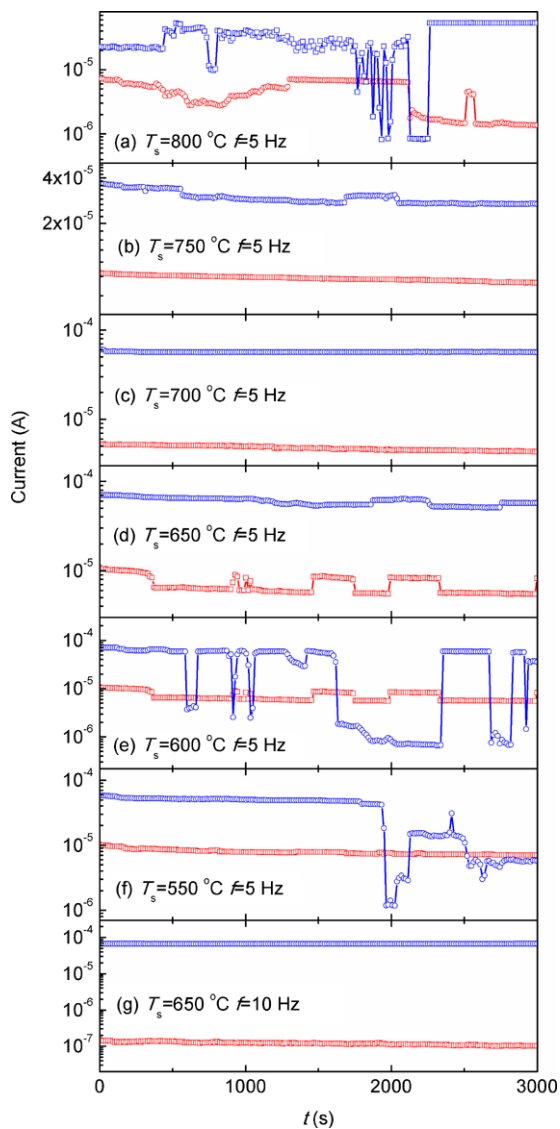


Fig. 6 Retention of the HRS and LRS at room temperature with reading voltage of 0.1 V for BiFeO₃ films prepared under different conditions

set process can be regarded as soft breakdown that the conducting filaments were formed between the top and bottom electrodes by the distribution of O vacancies under positive bias. However, in the reset process, the Joule heating might be not enough to rupture the filaments [28]. The negative bias can accelerate further migration of O vacancies away from the remaining filaments [29]. Furthermore, the Ag top electrode might act as an O reservoir which could provide sufficient O to neutralize the O vacancies during the reset process, which is helpful to the rupture of the filamentary conductive path, similar to the TiN electrode in TiN/ZnO/Pt device [30].

The retention property of the BRS in all the Ag/BiFeO₃/LaNiO₃ devices at room temperature is shown in Fig. 6. As can be seen, the HRS in all the devices is very stable. How-

ever, the LRS of the BiFeO₃ films prepared at T_s of 800 °C, 600 °C and 550 °C is unstable, and switching between HRS and LRS can be observed. These might be due to the high defects concentration in the BiFeO₃ films prepared at high and low T_s , the O vacancies in the conducting filaments might hopping between the neighboring sites, leading to the formation/rupture of the filaments. To increase the resistance ratio between HRS and LRS, increasing the bulk resistivity might be an efficient way, since the conducting filaments have the similar magnitude of resistivity. Shuai has reported that increasing the laser frequency will effectively increase the Bi concentration at the bottom interface and reduce the leakage current [16]. As can be seen in Fig. 6(g), the resistance of the BiFeO₃ film prepared with laser frequency of 10 Hz in LRS is comparable to the BiFeO₃ films prepared with laser frequency of 5 Hz, the resistance of HRS is almost 2 orders larger. The ratio between HRS to LRS is only about 10 in the BiFeO₃ films prepared with laser frequency of 5 Hz, which was enhanced to more than 2 orders in the BiFeO₃ film prepared with laser frequency of 10 Hz, and no degradation can be observed in both HRS and LRS with measuring time up to 3000 s. The large resistance ratio between HRS and LRS, and good retention properties make the BiFeO₃ film potential application in the non-volatile resistive random access memory.

4 Conclusions

In summary, pure-phase polycrystalline BiFeO₃ films have been successfully prepared by pulsed-laser deposition on surface oxidized Si substrates using LaNiO₃ buffer layer with T_s ranging from 550 °C to 800 °C and laser frequency of 5 Hz and 10 Hz. Bipolar resistive switching has been observed in all the films using LaNiO₃ as bottom electrodes and silver glue dots as top electrodes. The resistivity switches from HRS to LRS with positive voltage applied on the top Ag electrodes, and from LRS to HRS with positive voltage applied on the bottom LaNiO₃ electrodes. The mechanism of the resistive switching has been confirmed to be due to the voltage polarity dependent formation/rupture of the conducting filaments formed by the O vacancies. The highest resistive ratio of HRS to LRS of more than 2 orders of magnitude has been achieved in the highest resistive BiFeO₃ film prepared at T_s of 650 °C and laser frequency of 10 Hz, indicating the potential applications in the non-volatile resistive random access memory.

Acknowledgements This work is supported by the National Natural Science Foundation of China (50802041, 51172044), National Key Projects for Basic Researches of China (2010CB923404), the National Science Foundation of Jiangsu Province of China (BK2010421, BK2011617), by NCET-09-0296, Southeast University and the Scientific Research Foundation for the Returned Overseas Chinese Scholars, State Education Ministry.

References

1. Strukov, D.B., Snider, G.S., Stewart, D.R., Stanley Williams, R.: *Nature* **453**, 80 (2008) and references therein
2. Chua, L.: *Appl. Phys. A* **102**, 765 (2011)
3. Lee, S., Kim, H., Park, J., Yong, K.: *J. Appl. Phys.* **108**, 076101 (2010)
4. Chang, W., Lai, Y., Wu, T., Wang, S., Chen, F., Tsai, M.: *Appl. Phys. Lett.* **92**, 022110 (2008)
5. Nagashima, K., Yanagida, T., Oka, K., Kawai, T.: *Appl. Phys. Lett.* **94**, 242902 (2009)
6. Gao, X., Guo, H., Xia, Y., Yin, J., Liu, Z.: *Thin Solid Films* **519**, 450 (2010)
7. Kinoshita, K., Okutani, T., Tanaka, H., Hinoki, T., Yazawa, K., Ohmi, K., Kishida, S.: *Appl. Phys. Lett.* **96**, 143505 (2010)
8. Zhang, X.T., Yu, Q.X., Yao, Y.P., Li, X.G.: *Appl. Phys. Lett.* **97**, 222117 (2010)
9. Lee, W., Jo, G., Lee, S., Park, J., Jo, M., Lee, J., Jung, S., Kim, S., Shin, J., Park, S., Lee, T., Hwang, H.: *Appl. Phys. Lett.* **98**, 032105 (2011)
10. Wang, J., Neaton, J.B., Zheng, H., Nagarajan, V., Ogale, S.B., Liu, B., Viehland, D., Vaithyanathan, V., Schlom, D.G., Waghmare, U.V., Spaldin, N.A., Rabe, K.M., Wuttig, M., Ramesh, R.: *Science* **299**, 1719 (2003)
11. Lebeugle, D., Colson, D., Forget, A., Viret, M., Bonville, P., Marucco, J.F., Fusil, S.: *Phys. Rev. B* **76**, 024116 (2007)
12. Shuai, Y., Zhou, S., Streit, S., Reuther, H., Bürger, D., Slesazek, S., Mikolajick, T., Helm, M., Schmidt, H.: *Appl. Phys. Lett.* **98**, 232901 (2011)
13. Allibe, J., Infante, I.C., Fusil, S., Bouzehouane, K., Jacquet, E., Deranlot, C., Bibes, M., Barthélémy, A.: *Appl. Phys. Lett.* **95**, 182503 (2009)
14. Yin, K., Li, M., Liu, Y., He, C., Zhuge, F., Chen, B., Lu, W., Pan, X., Li, R.: *Appl. Phys. Lett.* **97**, 042101 (2010)
15. Li, M., Zhuge, F., Zhu, X., Yin, K., Wang, J., Liu, Y., He, C., Chen, B., Li, R.: *Nanotechnology* **21**, 425202 (2010)
16. Shuai, Y., Zhou, S., Bürger, D., Helm, M., Schmidt, H.: *J. Appl. Phys.* **109**, 124117 (2011)
17. Chen, X., Wu, G., Zhang, H., Qin, N., Wang, T., Wang, F., Shi, W., Bao, D.: *Appl. Phys. A* **100**, 987 (2010)
18. Chen, S., Wu, J.: *Thin Solid Films* **519**, 499 (2010)
19. Peng, H.Y., Li, G.P., Ye, J.Y., Wei, Z.P., Zhang, Z., Wang, D.D., Xing, G.Z., Wu, T.: *Appl. Phys. Lett.* **96**, 192113 (2010)
20. Ke, H., Wang, W., Wang, Y., Xu, J., Jia, D., Lu, Z., Zhou, Y.: *J. Alloys Compd.* **509**, 2192 (2011)
21. Liu, Z., Liu, H., Du, G., Zhang, J., Yao, K.: *J. Appl. Phys.* **100**, 044110 (2006)
22. Lee, M., Han, S., Jeon, S.H., Park, B.H., Kang, B.S., Ahn, S., Kim, K.H., Lee, C.B., Kim, C.J., Yoo, I., Seo, D.H., Li, X., Park, J., Lee, J., Park, Y.: *Nano Lett.* **9**, 1476 (2009)
23. Hu, Q., Jung, S.M., Lee, H.H., Kim, Y., Choi, Y.J., Kang, D., Kim, K., Yoon, T.: *J. Phys. D, Appl. Phys.* **44**, 085403 (2011)
24. Yan, Z., Guo, Y., Zhang, G., Liu, J.-M.: *Adv. Mater.* **23**, 1351 (2011)
25. Ji, Z., Mao, Q., Ke, W.: *Solid State Commun.* **150**, 1919 (2010)
26. Yang, Y.C., Pan, F., Liu, Q., Liu, M., Zeng, F.: *Nano Lett.* **9**, 1636 (2009)
27. Go, H., Wakiya, N., Funakubo, H., Satoh, K., Kondo, M., Cross, J.S., Maruyama, K., Mizutani, N., Shinozaki, K.: *Jpn. J. Appl. Phys.* **46**, 3491 (2007)
28. Lee, S., Kim, H., Park, J., Yong, K.: *J. Appl. Phys.* **108**, 076101 (2010)
29. Tsuruoka, T., Terabe, K., Hasegawa, T., Aono, M.: *Nanotechnology* **21**, 425205 (2010)
30. Xu, N., Liu, L.F., Sun, X., Chen, C., Wang, Y., Han, D.D., Liu, X.Y., Han, R.Q., Kang, J.F., Yu, B.: *Semicond. Sci. Technol.* **23**, 075019 (2008)